Inorg. Chem. **2003**, *42*, 5320–5329

Syntheses and Characterization of Titanium(IV) and Titanium(III) Complexes with (2-Dimethylphosphino)ethane-1-thiolate and (3-Dimethylphosphino)propane-1-thiolate as Ligands

Kazutaka Matsuzaki,[†] Hiroyuki Kawaguchi,[‡] Peter Voth,[†] Kyoko Noda,[§] Sumitaka Itoh,[§] Hideo D. Takagi,[†] Kazuo Kashiwabara,*[,§] and Kazuyuki Tatsumi[†]

Research Center for Materials Science and Department of Chemistry, Nagoya University, Nagoya 464-8602, Japan, and Institute for Molecular Science, Okazaki, Aichi, 444-8585 Japan

Received April 1, 2003

Reactions of Cp_2TiCl_2 (Cp = η^5-cyclopentadienide) with 2 or 1 equiv of hybrid P–S ligands (L), $(CH_3)_2P(CH_2)_nS^-$ (n = 2, dmpet; n = 3, dmppt), produced new dicyclopentadienyltitanium(IV) complexes with L, $Cp_2Ti(L\text{-}\kappa S)_2$ (**1**, L = dmpet; **2**, L = dmppt) and $[Cp_2Ti(L\text{-}\kappa^2S,P)]BPh_4$ (**3**, L = dmpet; **4**, L = dmppt). The Ti(III) complexes, $Cp_2Ti(L\text{-}\kappa^2S,P)$ (**5**, L = dmpet; **6**, L = dmppt), were prepared by the reaction of $Cp_2Ti(\eta^3\text{-}C_3H_5)$ with 1 equiv of L. The structures of complexes **1**–**6** were confirmed by X-ray diffraction analyses. It was found that complexes **3** and **5** were isostructural around Ti(IV) and Ti(III) centers: the Ti(IV)–S bond length in **3** (2.3498(9) Å) is shorter by 0.14 Å than Ti(III)–S in **5** (2.4877(7) Å), while Ti(IV)–P (2.534(1) Å) was merely 0.05 Å shorter than Ti(III)–P (2.5844(7) Å). The redox potential between **3** and **5** in acetonitrile was –1.14 V vs the ferricinium/ferrocene couple. A heterobimetallic complex that has the frame of complex **1**, $[Cp_2Ti(dmpet)_2Cu]PF_6$ (**7**), was also isolated and structurally characterized: the Ti–Cu distance (2.95(1) Å) was shorter than that in $[Cp_2Ti(SC_2H_4PPh_2)_2Cu]BF_4$, previously reported by White and Stephan. Structural characterization was also carried out for $Cp^*Ti(dmpet\text{-}\kappa S)_2(dmpet\text{-}\kappa^2S,P)$ (**8**) and $CpTiCl_2(dmppt\text{-}\kappa^2S,P)$ (**9**), which were obtained by the reactions of Cp*(or Cp)$TiCl_3$ (Cp^* = η^5-$C_5Me_5^-$) with n equiv (n = 1–3) of L. The mutual site-exchange reaction between phosphorus atoms on a coordinated dmpet in the κ^2S,P mode and on two other coordinated dmpet's in the κS mode within complex **8** was analyzed by the variable-temperature $^{31}P\{^1H\}$ dynamic NMR method. The kinetic parameters for this process, $k_{ex}^{298} = 1.9 \times 10^5$ s^{-1}, $\Delta H^{\ddagger} = 48$ kJ mol^{-1}, and $\Delta S^{\ddagger} = 17$ J mol^{-1} K^{-1}, as well as the rather long Ti(IV)–P distance (2.652(1) Å), indicate the fluxional nature of the coordination geometry in complex **8**.

Introduction

Although many metal complexes with diphenyl-substituted phosphine-thiol/thioether ligands, $Ph_2P(CH_2)_nSR$ (n = 2, 3), have been reported to date,[1−4] P−S ligands with a dimethyl-substituted phosphorus donor atom seem to have drawn little attention. Recent studies concerning syntheses and isomerization kinetics clearly indicated that the σ-donicity and π-acidity of phosphorus donor atoms are significantly altered by varying the substituents on the phosphorus atom:[5] methyl-substituted phosphines are somewhat strong σ-donors, while phenyl-substituted phosphines exhibit π-acidity, depending on the electronic configuration of the metal ion. We previously reported various metal complexes with hybrid P−S ligands, $(CH_3)_2PCH_2CH_2SR$ (R = H, Hdmpet; R = CH_3, mtdmpe), Ni(II), Pd(II), and Pt(II) complexes with dmpet[6] and mtdmpe,[7] and Co(III)[8] and Ru(II)[9] complexes

* Author to whom correspondence should be addressed. Tel/Fax: +81-52-789-5473. E-mail: kashiwa@chem.nagoya-u.ac.jp.
[†] Research Center for Materials Science, Nagoya University.
[‡] Institute for Molecular Science.
[§] Department of Chemistry, Nagoya University.

(1) Dilworth, J. R.; Wheatley, N. *Coord. Chem. Rev.* **2000**, *199*, 89−158.
(2) Hauptman, E.; Fagan, P.; Marshall, W. *Organometallics* **1999**, *18*, 2061−2073, and references therein.
(3) Morales, D.; Poli, R.; Richard, P.; Andrieu, J.; Collange, E. *J. Chem. Soc., Dalton Trans.* **1999**, 867−874.
(4) Brugat, N.; Polo, A.; Alvarez-Larena, A.; Piniella, J. F.; Real, J. *Inorg. Chem.* **1999**, *38*, 4829−4837, and references therein.
(5) Iwatsuki, S.; Suzuki, T.; Hasegawa, A.; Funahashi, S.; Kashiwabara, K.; Takagi, H. D. *J. Chem. Soc., Dalton Trans.* **2002**, 3593−3602.
(6) Kita, M.; Yamamoto, T.; Kashiwabara, K.; Fujita, J. *Bull. Chem. Soc. Jpn.* **1992**, *65*, 2272−2274.
(7) Suzuki, T.; Morikawa, A.; Kashiwabara, K. *Bull. Chem. Soc. Jpn.* **1996**, *69*, 2539−2548.

10.1021/ic034353l CCC: $25.00
Published on Web 07/29/2003

with mtdmpe, in which our intention was to examine the alteration in the coordination geometry around these electron-rich metal ions by introducing a $-PMe_2$ donor group instead of the popular $-PPh_2$ group since the steric requirements (Tolman's cone angle[10]) and the electronic effects (the basicity represented by pK_a of the conjugated acid and Tolman's χ parameter[11,12]) exhibited by these two phosphorus donor sites are very different from each other. It was found that the methyl substituents on the phosphorus donor site unequivocally induce a strong static trans influence that originates from the σ-donicity inherent in $-PMe_2$.

Studies concerning interactions between electron-deficient metal ions with a $-PMe_2$ donor site are still scarce, although examination of the coordination geometry of $[Mo(dmpet)_2(S^tBu)_2]$[13] and $(PPh_4)[W(S)_3(dmpet)]$[14] revealed that these compounds are excellent candidates for further syntheses of various heterometallic clusters. To further examine the nature of the interaction of hybrid P−S ligands with electron-deficient metal ions, a series of Ti(IV) (d^0) and Ti(III) (d^1) complexes with P−S hybrid ligands (dmpet or dmppt where dmppt = $(CH_3)_2PCH_2CH_2CH_2S^-$) were synthesized and the crystal structures were determined in this study, as such complexes have been limited to those reported by White and Stephan, $Cp_2Ti(SCH_2CH_2PPh_2)_2$[15] and $Cp_2Ti(SCH_2CH_2CH_2PPh_2)_2$,[16,17] in which the P−S ligand binds to Ti(IV) in a κS mode as a monodentate ligand. It was found that dmpet and dmppt ligands coordinate in a κ^2S,P mode at Ti(IV): only a few complexes with a Ti(IV)−phosphorus bond have been reported to date[18−30] because of the rather low coordinating ability of phosphines to electron-deficient Ti(IV). We also succeeded in isolating novel isostructural pairs of $[Cp_2Ti(dmpet\ or\ dmppt)]^{+/0}$. A heterobimetallic complex, $[Cp_2Ti(dmpet)_2Cu]PF_6$, similar to $[Cp_2Ti(SC_2H_4PPh_2)_2Cu]BF_4$ reported by White and Stephan,[15,17] was also isolated and structurally characterized. To explore the nature and reactivity of the bonding between phosphorus donor atoms and electron-deficient metal centers, we also examined the intramolecular site-exchange phenomenon in $[Cp^*Ti(dmpet)_3]$ in solution by means of variable-temperature $^{31}P\{^1H\}$ NMR.

Experimental Section

General Information. All reactions were carried out using standard Schlenk techniques under an argon atmosphere. Solvents were dried and distilled before use according to known methods. The following starting materials were prepared according to the literature methods: tetramethyldiphosphine,[31] Cp_2TiCl_2,[32] $Cp_2Ti(\eta^3\text{-}C_3H_5)$,[33] $[Cu(CH_3CN)_4]PF_6$,[34] $CpTiCl_3$,[35] and Cp^*TiCl_3.[36] The ^1H, $^{31}P\{^1H\}$, and $^{13}C\{^1H\}$ NMR spectra were recorded on a Varian UNITY plus-500 and Bruker AMX-400 WB spectrometers. IR and UV−visible spectra were measured by a Perkin-Elmer 2000FT-IR spectrophotometer and a JASCO-V560 spectrophotometer, respectively. EI-MS spectra were obtained on a Perkin-Elmer Sciex API-300. Elemental analyses were carried out on a LECO-CHNS microanalyzer, where the crystalline samples were sealed in thin silver tubes. A JES-RE IX X-band spectrometer was used for the measurements of the EPR spectra.

Electrochemical measurements were carried out by using a BAS 100B/W electrochemical analyzer at room temperature. Silver/silver nitrate in acetonitrile was used as the reference electrode, while a glassy carbon disk and a Pt wire were used as the working and counter electrodes, respectively. The redox potentials of sample solutions were calibrated by using the ferricinium/ferrocene redox signal. Tetra-*n*-butylammonium tetrafluoroborate (0.3 mol kg^{-1}) was used as the supporting electrolyte.

Synthesis of (2-Dimethylphosphino)ethane-1-thiol (Hdmpet). Hdmpet was prepared by the literature method.[6] ^1H NMR (C_6D_6): δ 2.36−2.27 (m, 2H, SC*H*$_2$), 1.40−1.34 (m, 3H, S*H* and C*H*$_2$P), 0.72 (d, 6H, P(C*H*$_3$)$_2$, J_{PH} = 2.5 Hz). $^{13}C\{^1H\}$ NMR (C_6D_6): δ 37.9 (d, S*C*H$_2$, J_{PC} = 14 Hz), 22.0 (d, *C*H$_2$P, J_{PC} = 20 Hz), 14.2 (d, P(*C*H$_3$)$_2$, J_{PC} = 15 Hz). $^{31}P\{^1H\}$ NMR (C_6D_6): δ −52.5. The white powder of Lidmpet was obtained almost quantitatively by mixing Hdmpet and ^{n}BuLi in hexane followed by the removal of solvent.

Synthesis of (3-Dimethylphosphino)propane-1-thiol (Hdmppt). Tetramethyldiphosphine (13.19 g, 108 mmol) was added to liquid ammonia (200 cm^3 at −78 °C) in a 500 cm^3 three-necked flask containing small pieces of metallic sodium (4.97 g, 216 mmol). After stirring the mixture for 3 h, 3-chloropropane-1-thiol (24.0 g, 217 mmol) was added. The solution was stirred for a further 1 h, followed by addition of 6 g of ammonium chloride (112 mmol). After 30 min, the solvent was evaporated at room temperature. The

(8) Kashiwabara, K.; Taguchi, N.; Takagi, H. D.; Nakajima, K.; Suzuki, T. *Polyhedron* **1998**, *17*, 1817−1829.
(9) Taguchi, N.; Kashiwabara, K.; Nakajima, K.; Kawaguchi, H.; Tatsumi, K. *J. Organomet. Chem.* **1999**, *587*, 290−298.
(10) Tolman, C. A. *Chem. Rev.* **1977**, *77*, 313−348.
(11) Streuli, C. A. *Anal. Chem.* **1960**, *32*, 985−987.
(12) Liu, H.; Eriks, K.; Prock, A.; Giering, W. *Organometallics* **1990**, *9*, 1758−1766, and references therein.
(13) Arikawa, Y.; Kawaguchi, H.; Kashiwabara, K.; Tatsumi, K. *Inorg. Chem.* **1999**, *38*, 4549−4553.
(14) Arikawa, Y.; Kawaguchi H.; Kashiwabara, K.; Tatsumi, K. *Inorg. Chem.* **2002**, *41*, 513−520.
(15) White, G. S.; Stephan, D. W. *Inorg. Chem.* **1985**, *24*, 1499−1503.
(16) White, G. S.; Stephan, D. W. *Organometallics* **1987**, *6*, 2169−2175.
(17) White, G. S.; Stephan, D. W. *Organometallics* **1988**, *7*, 903−910.
(18) Bottrill, M.; Gavens, P. D.; Kelland, J. W.; McMeeking, J. In *Comprehensive Organometallic Chemistry*; Wilkinson, G., Stone, F. G. A., Abel, E. W., Eds.; Pergamon Press: Oxford, 1982; Vol. 5, Chapter 22.
(19) Bochman, M. In *Comprehensive Organometallic Chemistry II*; Abel, E. W., Stone, F. G. A., Wilkinson, G., Eds.; Pergamon Press: Oxford, 1995; Vol. 4, Chapters 4 and 5.
(20) Cotton, F. A.; Murillo, C. A.; Petrukhina. M. A. *J. Organomet. Chem.* **2000**, *593*, 1−6.
(21) Cotton, F. A.; Murillo, C. A.; Petrukhina. M. A. *J. Organomet. Chem.* **1999**, *573*, 78−86.
(22) Cotton, F. A.; Petrukhina, M. A. *Inorg. Chem. Commun.* **1998**, *1*, 195−196.
(23) Willoughby, C. A.; Duff, R. R., Jr.; Davies, W. M.; Buchwald, S. L. *Organometallics* **1996**, *15*, 472−475.
(24) Chadwell, S. J.; Coles, S. J.; Edwards, P. G.; Hursthouse, M. B. *J. Chem. Soc., Dalton Trans.* **1996**, 1105−1112.
(25) Pulst, S.; Arndt, P.; Baumann, W.; Tillack, A.; Kempe, R.; Rosenthal, U. *J. Chem. Soc., Chem. Commun.* **1995**, 1753−1754.
(26) Noth, H.; Schmidt, M. *Organometallics* **1995**, *14*, 4601−4610.
(27) Doxsee, K. M.; Garner, L. C.; Juliette, J. J. J.; Mouser, J. K. M.; Weakley, J. R.; Hope, H. *Tetrahedron* **1995**, *51*, 4321−4332.
(28) Nadasdi, T.; Stephan, D. W. *Inorg. Chem.* **1993**, *32*, 5933−5938.
(29) Park, J. W.; Henling, L. M.; Schaefer, W. P.; Grubbs, R. H. *Orgametallics* **1990**, *9*, 1650−1656.
(30) Hues, D. L.; Leigh, G. J.; Walker, D. G. *J. Organomet. Chem.* **1988**, *355*, 113−119.
(31) Butter, S. A.; Chatt, J. *Inorg. Synth.* **1974**, *15*, 185−191.
(32) Wilkinson, G.; Birmingham, J. M. *J. Am. Chem. Soc.* **1954**, *76*, 4281−4284.
(33) Martin, H. A.; Jellinek, F. J. *Organomet. Chem.* **1967**, *8*, 115−128.
(34) Kubas, G. J. *Inorg. Synth.* **1979**, *19*, 90−92.
(35) King, R. B. *Organometallic Syntheses*; Academic: New York, 1965; Vol. 1, p 78.
(36) Yamamoto, H.; Yasuda, H.; Tatsumi, K.; Lee, K.; Nakamura, A.; Chen, J.; Kai, Y.; Kasai, N. *Organometallics* **1989**, *8*, 105−119.

product was then extracted by diethyl ether from the residue. Evaporation of ether under reduced pressure after filtration gave a colorless oily product, which was distilled (bp 30−35 °C/2 mmHg) to obtain pure Hdmppt as a clear liquid. The yield was 10.98 g (37%). ^{1}H NMR (C_6D_6): δ 2.23 (dt, 2H, SCH_2), 1.49 (m, 2H, $CH_2CH_2CH_2$), 1.13 (m, 1H, SH), 1.13 (m, 2H, CH_2P), 0.80 (d, 6H, P(CH_3)$_2$, J_{PH} = 2.7 Hz). ^{13}C{^{1}H} NMR (C_6D_6): δ 31.5 (d, SCH_2, J_{PC} = 11.5 Hz), 31.1 (d, CH_2P, J_{PC} = 14.4 Hz), 26.5 (d, CH_2CH_2-CH_2, J_{PC} = 12.7 Hz), 14.5 (d, P(CH_3)$_2$, J_{PC} = 14.4 Hz). ^{31}P{^{1}H} NMR (C_6D_6): δ −52.8.

Synthesis of Cp$_2$Ti(dmpet)$_2$ (1). A THF solution (45 cm^3) of Cp_2TiCl_2 (306 mg, 1.23 mmol) was added to a suspension of Lidmpet (2.90 mmol) in THF (15 cm^3) at 0 °C. The mixture was stirred for 1 h at room temperature, and the solvent was removed under reduced pressure. The extract with diethyl ether (40 cm^3) from the deep purple residue was concentrated to ca. 5 cm^3 and cooled to −30 °C, yielding purple crystals of **1** (770 mg, 87%). Prismatic red-purple crystals were obtained by recrystallization from hexane at −10 °C. ^{1}H NMR (C_6D_6): δ 5.77 (s, 10H, C_5H_5), 3.39 (m, 4H, SCH_2), 1.79 (m, 4H, CH_2P), 0.98 (d, 12H, P(CH_3)$_2$, J_{PH} = 2.7 Hz). ^{31}P{^{1}H} NMR (C_6D_6): δ −50.9. IR (Nujol mull/KBr): 3150 w, 1430 m, 1283 m, 933 s, 880 m, 835 m, 810 s cm^{-1}. UV−visible (λ_{max}/nm (ϵ/M^{-1} cm^{-1}), hexane): 540 (2600), 364 (2700). Anal. Calcd for $C_{18}H_{30}P_2S_2Ti$: C, 51.43; H, 7.19; S, 15.26. Found: C, 51.21; H, 7.02; S, 15.32.

Synthesis of Cp$_2$Ti(dmppt)$_2$ (2). The preparation was carried out by the method similar to that used for the synthesis of **1**. Extraction was carried out with hexane, instead of diethyl ether, which was used for the synthesis of **1**. The yield was 91%. ^{1}H NMR (C_6D_6): δ 5.87 (s, 10H, C_5H_5), 3.38 (m, 4H, SCH_2), 1.56 (m, 4H, $CH_2CH_2CH_2$), 1.93 (m, 4H, CH_2P), 0.98 (d, 12H, P(CH_3)$_2$, J_{PH} = 2.7 Hz). ^{31}P{^{1}H} NMR (C_6D_6): δ −53.0. IR (Nujol mull/KBr): 3060 w, 1284 m, 1019 s, 941 m, 815 s, 722 m cm^{-1}. UV−visible (λ_{max}/nm, hexane): 539. Anal. Calcd for $C_{20}H_{34}P_2S_2Ti$: C, 53.57; H, 7.74; S, 14.30. Found: C, 53.03; H, 7.94; S, 13.77.

Synthesis of [Cp$_2$Ti(dmpet)]B(C$_6$H$_5$)$_4$ (3). Lidmpet (1.01 mmol) in THF (30 cm^3) was added to Cp_2TiCl_2 (250 mg, 1.01 mmol) in THF (40 cm^3) at 0 °C. The dark red solution was stirred for 2 h at room temperature, and the solvent was evaporated under reduced pressure. The dark red residue was extracted with toluene (40 cm^3), followed by evaporation of the solvent. The residue was redissolved in 30 cm^3 of THF, and a THF solution of $NaBPh_4$ (274 mg, 0.80 mmol) was added. After stirring the mixture overnight, a purple crystalline powder was precipitated, which was dissolved in acetonitrile, and insoluble solids were removed by centrifugation. The clear solution was concentrated and cooled to −30 °C, yielding purple crystals of **3**·CH_3CN. (180 mg, 34%). ^{1}H NMR (CD_3CN): δ 7.28 (m, 8H, BPh_4), 7.01 (m, 8H, BPh_4), 6.83 (m, 4H, BPh_4), 6.57 (d, 10H, C_5H_5, J_{PH} = 2.7 Hz), 4.01 (m, 2H, SCH_2), 3.19 (m, 2H, CH_2P), 1.51 (d, 6H, P(CH_3)$_2$, J_{PH} = 9.8 Hz). ^{31}P{^{1}H} NMR (CD_3CN): δ 22.6. IR (Nujol mull/KBr): 3110 m, 3050 m, 1580 m, 1428 m, 1260 s, 950 s, 928 m, 900 m, 846 m, 828 s, 752 s, 738 s, 714 s, 600 s, 485 w, 465 w cm^{-1}. UV−visible (λ/nm (ϵ/M^{-1} cm^{-1}), CH_3CN): 545 (2400), 390 (sh), 332 (8000). EI-MS (*m*/*z*, CH_3CN): 299 ([Cp$_2$Ti(dmpet)]$^+$). Anal. Calcd for $C_{40}H_{43}BNPSTi$: C, 72.85; H, 6.57; S, 4.86. Found: C, 71.95; H, 6.46; S, 4.51.

Synthesis of [Cp$_2$Ti(dmppt)]B(C$_6$H$_5$)$_4$ (4). The preparation was carried out by a method similar to that for **3**. After removal of THF, a red crystalline powder was obtained. The crude compound was recrystallized from CH_3CN/diethyl ether. The yield was 82%. ^{1}H NMR (CD_3CN): δ 7.28 (m, 8H, BPh_4), 7.01 (m, 8H, BPh_4), 6.83 (m, 4H, BPh_4), 6.45 (d, 5H, C_5H_5, J_{PH} = 2.4 Hz), 6.25 (d, 5H, C_5H_5, J_{PH} = 2.7 Hz), 4.22 (m, 1H, SCH_2), 3.80 (m, 1H, SCH_2), 2.59 (m, 1H, CH_2P), 2.43 (m, 1H, CH_2P), 1.51 (d, 3H, P(CH_3), J_{PH} = 9.8 Hz), 1.21 (d, 3H, P(CH_3), J_{PH} = 8.8 Hz), 1.08 (m, 2H, $CH_2CH_2CH_2$). ^{31}P{^{1}H} NMR (CD_3CN): δ 24.2. IR (Nujol mull/KBr): 3100 w, 3040 w, 1576 s, 1424 m, 1272 s, 1260 m, 942 s, 925 s, 842 s, 825 s, 735 s, 710 s, 628 s, 610 s, 482 m, 464 m cm^{-1}. UV−visible (λ/nm (ϵ/M^{-1} cm^{-1}), CH_3CN): 492 (1000), 330 (8000). EI-MS (*m*/*z*, CH_3CN): 313 ([Cp$_2$Ti(dmppt)]$^+$). Anal. Calcd for $C_{39}H_{42}BPSTi$: C, 74.06; H, 6.70; S, 5.07. Found: C, 73.39; H, 6.73; S, 4.95.

Synthesis of Cp$_2$Ti(dmpet) (5). Hdmpet (144 mg, 1.18 mmol) was added to the THF solution (30 cm^3) of Cp$_2$Ti(η^3-C_3H_5) (247 mg, 1.06 mmol). The color of the solution changed immediately from reddish purple to dark green. After stirring the mixture for 0.5 h, the solution was concentrated to ca. 5 cm^3 and cooled to −30 °C, yielding dark red crystals of **5** (245 mg, 77%). IR (Nujol mull/KBr): 3100 w, 1435 w, 1283 s, 959 s, 870 m, 795 s cm^{-1}. Anal. Calcd for $C_{14}H_{20}PSTi$: C, 56.20; H, 6.74; S, 10.72. Found: C, 55.70; H, 6.75; S, 10.46.

Synthesis of Cp$_2$Ti(dmppt) (6). Preparation of **6** was carried out by a method similar to that used for the synthesis of **5**. Yield: 56%. IR (Nujol mull/KBr): 3060 w, 1260 w, 946 m, 870 m, 795 s cm^{-1}. Anal. Calcd for $C_{15}H_{22}PSTi$: C, 57.51; H, 7.08; S, 10.24. Found: C, 56.92; H, 7.39; S, 10.22.

Synthesis of [Cp$_2$Ti(dmpet)$_2$Cu]PF$_6$ (7). To a CH_3CN solution (40 cm^3) of [Cu(CH_3CN)$_4$]PF_6 (0.17 g, 0.456 mmol) was slowly added a CH_3CN solution (20 cm^3) of **1**. The dark red mixture was stirred for a further 4 h and then concentrated to ca. 5 cm^3. Diethyl ether was slowly added to the concentrate, yielding a dark red crystalline powder of **7**, which was washed with diethyl ether (20 cm^3 × 2). The yield was 84%. ^{1}H NMR (CD_3CN): δ 5.98 (s, 10H, C_5H_5), 3.31 (br, 4H, SCH_2), 2.10 (br, 4H, CH_2P), 1.35 (d, 12H, P(CH_3), J_{PH} = 2.7 Hz). ^{31}P{^{1}H} NMR (CD_3CN): δ −21.6 (*P*Me$_2$), −143.2 (quint., *P*F$_6$, J_{PF} = 707 Hz). IR (Nujol mull/KBr): 3120 w, 1425 m, 1410 w, 1395 w, 1285 m, 1260 w, 1245 w, 953 s, 930 s, 802 s cm^{-1}. UV−visible (λ/nm (ϵ/M^{-1} cm^{-1}), CH_3CN): 405 (8900). Anal. Calcd for $C_{18}H_{30}CuF_6P_3S_2Ti$: C, 34.38; H, 4.81; S, 10.20. Found: C, 34.82; H, 4.92; S, 10.40.

Attempts to isolate and characterize heterobimetallic complexes with Fe(II) or Ni(II) were not successful. Reactions of **1** with $NiCl_2$-(PPh_3)$_2$ and $FeCl_2$ produced only Ni(dmpet)$_2$[6] (ca. 94% yield) and Fe_3(dmpet)$_6$Cl (ca. 59% yield), respectively. The reaction of **2** with Ni(cod)$_2$ (cod = 1,5-cyclooctadiene) yielded merely a trace amount of [Cp$_2$Ti($SC_3H_6PMe_2$)$_2$Ni], which is in contrast to the high yield of [Cp$_2$Ti($SC_3H_6PPh_2$)$_2$Ni][17] (70%). The dark green solid, obtained after removing the solvent from the reaction mixture, contained several nonidentifiable byproducts according to the ^{31}P{^{1}H} and ^{1}H NMR spectra. On the other hand, [Ni(dmppt)$_2$] was isolated (ca. 50% yield) from the reddish brown mixture of **2** and Ni(cod)$_2$ in THF. The reactions of **2** with $FeCl_2$ and [Fe(CH_3CN)$_6$](ClO$_4$)$_2$ yielded only Fe_3(dmppt)$_6$Cl and [Fe_2(dmppt)$_3$(CH_3CN)$_3$](ClO$_4$)$_2$, respectively.

Synthesis of Cp*Ti(dmpet)$_3$ (8). Cp*$TiCl_3$ (360 mg, 1.24 mmol) in THF (20 cm^3) was added to a suspension of Lidmpet (3.8 mmol) in THF (15 cm^3) at 0 °C. The dark red solution was stirred at room temperature for 1 h, followed by the removal of the solvent. The residue was extracted with hexane (50 cm^3), and the extract was filtered. The filtrate was concentrated to ca. 5 cm^3 and cooled to −30 °C, yielding red crystals. (430 mg, 63%). ^{1}H NMR (C_6D_6): δ 3.62−3.35 (m, 6H, SCH_2), 2.14 (s, 15H, C_5(CH_3)$_5$), 1.94−1.73 (m, 6H, CH_2P), 1.12 (d, 18H, P(CH_3)$_2$, J_{PH} = 1.7 Hz). ^{31}P{^{1}H} NMR (C_6D_6, 80 °C): δ −29 (br). IR (Nujol mull/KBr): 1430 w, 1285 m, 932 s, 788 (br) cm^{-1}. UV−visible (λ/nm, hexane): 435, 374.

Table 1. Crystallographic Data for **1**−**9**

	1	**2**	**3**	**4**	**5**	**6**	**7**	**8**	**9**
formula	$C_{18}H_{30}P_2S_2Ti$	$C_{20}H_{34}P_2S_2Ti$	$C_{40}H_{43}BNPSTi$	$C_{39}H_{42}BPSTi$	$C_{14}H_{20}PSTi$	$C_{15}H_{22}PSTi$	$C_{18}H_{30}CuF_6P_3S_2Ti$	$C_{22}H_{45}P_3S_3Ti$	$C_{10}H_{17}Cl_2PSTi$
fw	420.40	448.46	659.53	632.50	299.25	313.27	628.91	546.60	319.08
temp (K)	296.2	296.2	296.2	296.2	296.2	296.2	296.2	296.2	273.2
space group	triclinic	triclinic	triclinic	orthorhombic	monoclinic	monoclinic	orthorhombic	triclinic	monoclinic
	$P\bar{1}$ (2)	$P\bar{1}$ (2)	$P\bar{1}$ (2)	$Pna2_1$ (33)	$P12_1/n1$ (14)	$P12_1/a1$ (14)	$Pna2_1$ (33)	$P\bar{1}$ (2)	$P12_1/n1$ (14)
a (Å)	11.579(4)	11.432(2)	12.855(4)	29.621(5)	8.059(2)	15.692(2)	25.796(2)	13.359(3)	7.216(1)
b (Å)	13.098(4)	13.193(3)	13.828(6)	9.772(5)	15.155(3)	13.804(4)	9.973(2)	14.035(3)	13.970(3)
c (Å)	8.159(2)	8.755(2)	10.223(3)	11.557(4)	12.164(2)	16.223(5)	9.943(2)	8.586(3)	13.8178(7)
α (deg)	91.44(2)	103.68(2)	91.09(3)	90	90	90	89	106.74(2)	90
β (deg)	108.58(2)	94.68(1)	100.13(2)	90	102.55(2)	117.92(2)	89	106.56(2)	103.574(1)
γ (deg)	107.08(3)	70.36(1)	78.52(3)	90	90	90	90	89.84(2)	90
V (Å^3)	1111.5(7)	1208.3(4)	1752(1)	3345(3)	1450.1(5)	3105(1)	2557(1)	1472.1(7)	1354.0(3)
Z	2	2	2	4	4	8	4	2	4
D_{calcd} (g cm^{-3})	1.256	1.232	1.250	1.256	1.371	1.340	1.633	1.233	1.565
μ(Mo Kα) (cm^{-1})	0.714	0.661	0.378	0.393	0.821	0.770	1.543	0.675	1.265
R	0.051	0.044	0.038	0.086	0.032	0.049	0.044	0.055	0.039
R_w	0.0507	0.0507	0.0430	0.0790	0.0396	0.0498	0.0497	0.0746	0.0514

Anal. Calcd for $C_{22}H_{45}TiS_3P_3$: C, 48.34; H, 8.30; S, 17.60. Found: C, 48.21; H, 8.09; S, 17.27.

Synthesis of CpTiCl$_2$(dmppt) (9). Lidmppt (1.0 mmol) in THF (15 cm^3) was added to a THF solution (20 cm^3) of $CpTiCl_3$ (215 mg, 1.0 mmol) at 0 °C, and the mixture was stirred for 2 h. After removal of the solvent, the green oily residue was extracted with 1,2-dimethoxyethane (DME). The DME solution was concentrated and cooled to −30 °C, yielding green crystals of **9** (177 mg, 57%). ^{1}H NMR ($CDCl_3$): δ 6.56 (d, 5H, C_5H_5, J_{PH} = 2.4 Hz), 3.70 (br m, 2H, SCH_2), 2.29 (br m, 2H, CH_2P), 1.86 (br m, 2H, CH_2CH_2-CH_2), 1.49 (d, 6H, $P(CH_3)_2$, J_{PH} = 9.3 Hz). ^{31}P{^{1}H} NMR ($CDCl_3$): δ 13.22. EI-MS (m/z): 319 ($CpTiCl_2(dmppt)^+$), 283 ($CpTiCl_2(dmppt)^+Cl^-$), 218 ($TiCl(dmppt)_2^+$). Anal. Calcd for $C_{10}H_{17}Cl_2PSTi$: C, 37.64; H, 5.37; S, 10.05. Found: C, 37.21; H, 5.07; S, 9.64.

Crystal Structure Determinations. Crystallographic parameters for **1**−**9** are summarized in Table 1. Single crystals were obtained as described in the Experimental Section. The crystals suitable for X-ray analyses were mounted in glass capillaries and sealed under argon. Diffraction data of compounds except for **9** were collected at room temperature on a Rigaku AFC7R diffractometer with graphite-monochromated Mo Kα radiation (λ = 0.710690 Å) using the $\omega-2\theta$ scan technique. Refined cell dimensions and their standard deviations were obtained by the least-squares method with 25 randomly selected centered reflections. These standard reflections, monitored periodically for crystal decomposition or movement, exhibited slight intensity variation over the course of the data collections. The raw intensities were corrected for Lorentz and polarization effects. Empirical absorption corrections based on Ψ scans were applied.

Data collections of **9** were carried out on a Rigaku AFC7 equipped with a MSC/ADSC Quantum 1 CCD detector at room temperature. Four preliminary data frames were measured at 0.5° increments of ω, to assess the crystal quality and calculate preliminary unit cell parameters. The intensity image was measured at 0.5° intervals of ω for a duration of 82 s for **9**. The frame data were integrated using the d*TREK program package, and the data sets were corrected empirically for absorption using the REQAB program.

All calculations were carried out by using the TEXSAN program package. All structures were solved by direct methods, and then the structures were refined by full-matrix least-squares analyses. Anisotropic refinement was applied to all non-hydrogen atoms, and all the hydrogen atoms were placed at calculated positions. For **1**, one methyl group and one P atom of dmpet are disordered with occupancy factors of 83:17. Additional information is available as Supporting Information.

Scheme 1

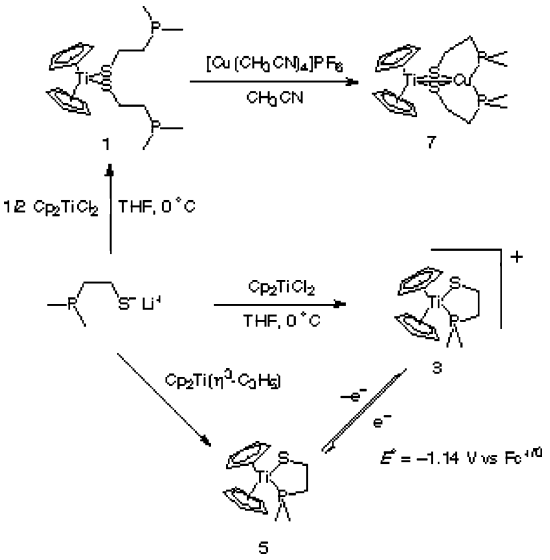

Results and Discussion

A schematic diagram for the syntheses of complexes **1**, **3**, **5**, and **7** is shown in Scheme 1. The synthetic routes for the corresponding dmppt complexes **2**, **4**, and **6** can be described by a similar scheme.

Ti(IV) Complexes of Cp$_2$TiL$_2$ and [Cp$_2$TiL]BPh$_4$ (L = dmpet and dmppt). Complexes **1** and **2** were obtained by the reactions of Cp_2TiCl_2 with 2 equiv of Lidmpet and Lidmppt, respectively, in ca. 90% yields. Reactions of Cp_2TiCl_2 with 1 equiv of Lidmpet and Lidmppt produced complexes **3** and **4**, respectively, in moderate yields, 35−80%. It was not possible to isolate $Cp_2TiCl(dmpet)$, the probable precursor of **3**.

The crystal structures of **1**, **2**, **3**, and **4** were determined by X-ray diffraction methods. ORTEP drawings of the molecular structures of **1** and **2** and the cationic parts of **3** and **4** are shown in Figure 1 with selected bond lengths (Å)

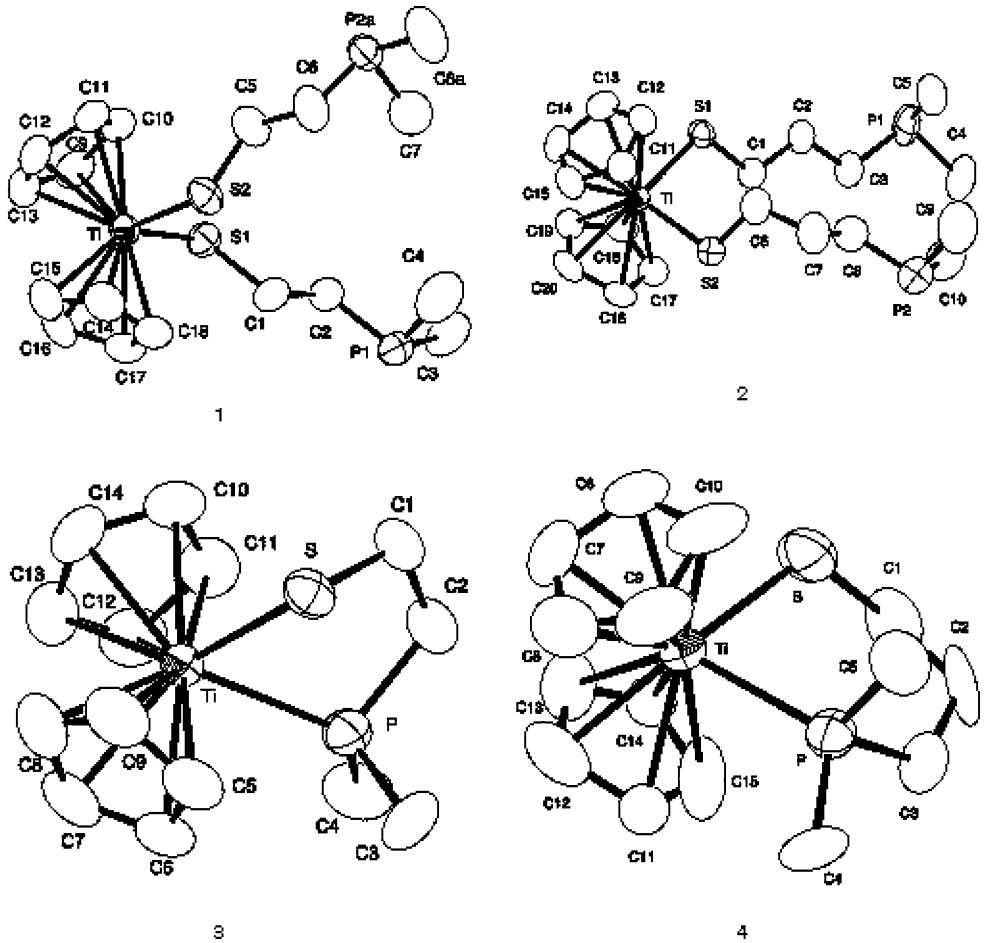

Figure 1. ORTEP drawings of **1** (Ti−S(1) 2.390(2), Ti−S(2) 2.383(3) Å, S(1)−Ti−S(2) 93.62(8)°) and **2** (Ti−S(1) 2.387(1), Ti−S(2) 2.397(1) Å, S(1)−Ti−S(2) 94.74(4)°), and the cationic parts of **3** (Ti−S 2.3498(9), Ti−P 2.534(1) Å, S−Ti−P 72.63(3)°) and **4** (Ti−S 2.332(9), Ti−P 2.54(2) Å, S−Ti−P 79.7(5)°).

and angles (deg). The dmpet and dmppt in **1** and **2** coordinate to the Ti(IV) center as a monodentate ligand through S, whereas those in **3** and **4** bind to the Ti(IV) center with both phosphorus and sulfur atoms. The Ti−S bond lengths and the S−Ti−S bond angles in **1** and **2** are almost identical to those (2.378(6) and 2.384(6) Å, and 93.3(2)°) in $Cp_2Ti(SCH_2CH_2CH_2PPh_2)_2$, which was reported by White and Stephan.[16] The $^{31}P\{^1H\}$NMR spectra of **1** and **2** in C_6D_6 exhibited sharp singlet signals at −50.9 and −53.0 ppm, respectively. These values are close to those for the free ligands, −52.5 (Hdmpet) and −52.8 ppm (Hdmppt) in C_6D_6, indicating no coordination of phosphorus donor atoms in solution. On the other hand, the $^{31}P\{^1H\}$NMR spectra of **3** and **4** in CD_3CN exhibited singlet signals at 22.6 and 24.2 ppm, respectively. The large downfield shifts (75−77 ppm) of the $^{31}P\{^1H\}$NMR signals of the $-P(Me)_2$ group confirm the coordination of dmpet and dmppt through both phosphorus and sulfur atoms: the structures observed in the solid state are retained in solution.[37] The ^1H NMR spectra of **3** and **4** also confirmed the observations by the $^{31}P\{^1H\}$NMR method. All signals due to the Cp moieties in **3** and **4** appeared as doublets: a doublet signal with $J_{PH} = 2.7$ Hz for **3** and two doublet signals with $J_{PH} = 2.4$ and 2.7 Hz for **4**. Nonequivalence of the two Cp rings in **4** may be attributed to the fixed chair conformation of the dmppt chelate ring, which is very much like that observed for Cp_2Ti(dmppt) **6**, while the flexibility of the distorted gauche (envelope) conformation of the dmpet chelate ring in **3** readily provides an equivalent environment for the two Cp rings in **3**. The rigidity of the dmppt chelate ring in **4** stems from (1) the significant steric congestion around Ti(IV) in **4** as discussed below and (2) the large energy barrier for the inversion.

Complexes **3** and **4** are rare examples of Cp_2Ti(IV) species with a Ti−phosphorus bond.[25,29] The Ti(IV)−P bond length in **3**, 2.534(1) Å, is notably shorter than those in $Cp_2Ti(\eta^2\text{-}CH_2S)(PMe_3)$[29](2.601(1) Å) and $[Cp_2Ti(\eta^2\text{-}CH_2SMe)(PMe_3)]I$[29] (2.581(1) Å), although it is similar to the $Ti-PPh_2$ bond length in the phosphide-bridged $Cp_2Ti(\mu\text{-}\sigma,\eta^2\text{-}CCPh)(\mu\text{-}PPh_2)Ni(PPh_3)$[25] (2.516(2) Å). The Ti(IV)−P bond found in **3** is the shortest of all of the reported analogous complexes in which the Ti(IV)−phosphine bonds are in the range 2.57−2.65 Å.[20−30] The Ti(IV)−S bond length in **3** (2.3498(9) Å) is shorter by ca. 0.04 Å than that (av 2.387(2) Å) in **1**, probably because of the positive charge on the cationic part of **3**. The Ti(IV)−S and Ti(IV)−P bond lengths in **4** are similar to those in complex **3**, while the S−Ti(IV)−P angle was wider in **4** (79.7°) than in **3** (72.6°), reflecting the larger bite angle of the dmppt ligand. However, relatively small S−Ti(IV)−P angles (≪90°) as well as the long Ti(IV)−P

(37) Garrou, P. E. *Chem. Rev.* **1981**, *81*, 229−266.

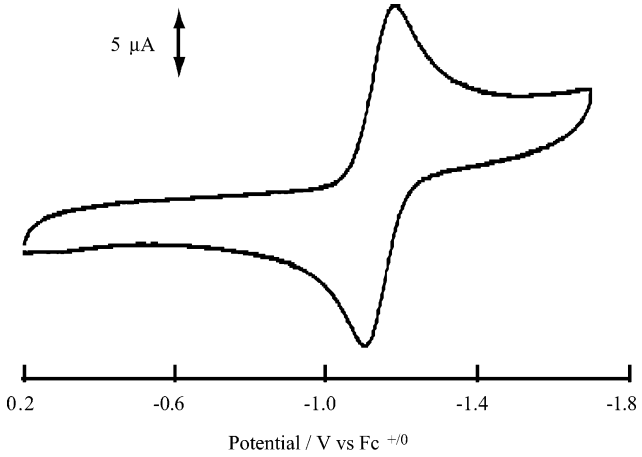

Figure 2. Cyclic voltammogram of the $[Cp_2Ti(dmpet)]^{+/0}$ couple in acetonitrile. $[Cp_2Ti(dmpet)BPh_4] = 1.3 \times 10^{-3}$ mol kg^{-1}. Sweep rate is 0.1 V s^{-1}. T = room temperature. $I = 0.3$ mol kg^{-1}($TBABF_4$).

bond lengths in these complexes indicate that the coordination environment around Ti(IV) in these complexes is sterically congested because of the two Cp groups and that the Ti(IV)−P bonds in these complexes are rather weak.

The redox potential of the $[Cp_2Ti(dmpet)]^{+/0}$ couple was measured in acetonitrile. As shown in Figure 2, the voltammogram was quasi-reversible with $E_{p-p} = 96$ mV and $I_{cathodic}/I_{anodic} \approx 1.0$. No other signal was observed within the experimental potential window, from −2.0 to +1.0 V. Therefore, the redox potential for the $[Cp_2Ti(dmpet)]^{+/0}$ couple was determined as −1.14 V vs the ferricinium/ferrocene couple. Such a low redox potential confirms the instability of the Ti(III) oxidation state as described in the Experimental Section. However, the quasi-reversible signals of the voltammogram even at a slower scan rate than 100 mV s^{-1} indicates that the Ti(III) complex is not labile. Therefore, it seems possible to isolate the corresponding Ti(III)-dmpet complex, although it is predicted that such a species is highly air-sensitive. We will report the successful isolation and characterization of $[Cp_2Ti^{III}(dmpet)]$ in the next section.

Complexes **1** and **2** are somewhat unstable upon exposure to air due to the oxidation of the dangling $-PMe_2$ moieties, while complexes **3** and **4** are considerably resistant to air-oxidation. Both **3** and **4** did not react with acetone, benzaldehyde, and methanol. However, they decomposed gradually in the presence of water. The reaction of **3** dissolved in CH_3CN with 1 equiv of Lidmpet in THF at 0 °C gave **1** in a 61% yield. The reaction of **1** in THF with 3 equiv of MeI produced $[Cp_2Ti(dmpetMe)_2]I_2$ in a 78% yield, while the formation of the phosphonium salt was confirmed by the $^{31}P\{^1H\}$ NMR (27.3 ppm) and ^1H NMR (δ 1.90, d (J_{PH} = 14 Hz), 18H, $-P(CH_3)_3$) spectra and elemental analysis. A similar reaction was also reported for $Cp_2Ti(SC_2H_4PPh_2)_2$ by White and Stephan.[15] We also examined the catalytic activity of **1** for the ethylene polymerization reaction with excess MAO (methylaluminoxane): 1.58×10^5 g (mol Ti)$^{-1}$ h^{-1} at 50 °C in toluene. The number average molecular weight, M_n, was 2.75×10^5, and M_w/M_n was 2.27, indicating that the thiol ligand in **1** is readily substituted by a methyl anion from MAO and by olefins. The catalytic activity was the largest for **1**, and it was not significant for all the other complexes. Moreover, the catalytic activity of **1** was well below the performance of other standard catalysts.

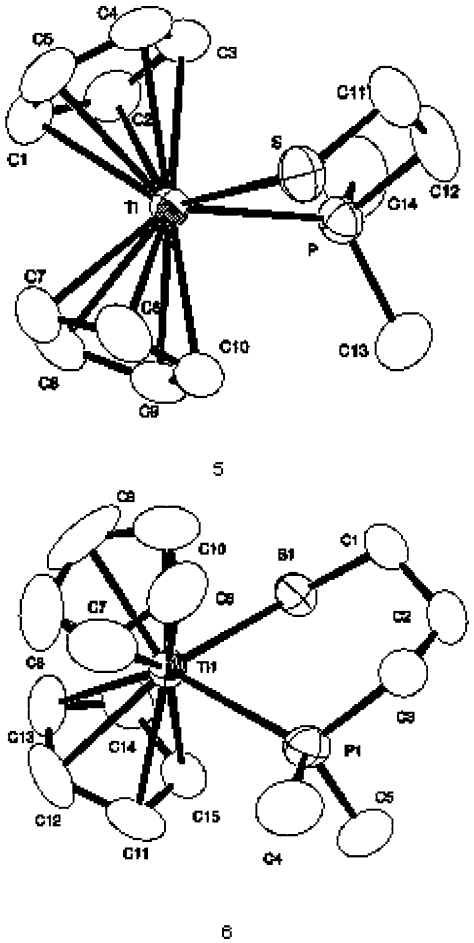

Figure 3. ORTEP drawings of **5** (Ti−S 2.4877(7), Ti−P 2.5844(7) Å, S−Ti−P 74.71(2)°) and **6** (Ti−S 2.503(2), Ti−P 2.568(2) Å, S−Ti−P 79.22(6)°).

Ti(III) Complexes of Cp_2TiL (L = dmpet and dmppt). Complexes **5** and **6**, Cp_2Ti(dmpet or dmppt), were prepared by the reactions of $Cp_2Ti(\eta^3\text{-}C_3H_5)$ with 1 equiv of Hdmpet or Hdmppt, in 60−80% yields (Scheme 1). Both complexes are highly sensitive to air and moisture, in contrast to **3** and **4**, as predicted by the very low redox potential for the $[Cp_2Ti(dmpet)]^{+/0}$ couple in acetonitrile (see Figure 2).

According to the X-ray crystallographic analyses, there are two independent molecules of **6** in an asymmetric unit. The ORTEP drawings of **5** and one of two molecules in **6** are shown in Figure 3 with the selected bond lengths and angles. The dmpet and dmppt ligands in **5** and **6** coordinate to the Ti(III) center through both phosphorus and sulfur atoms and form a distorted gauche and a typical chair conformation, respectively. Complexes **5** and **3** exhibited identical coordination geometry. The Ti(III)−S and Ti(III)−P bond lengths in **5** are 2.4877(7) and 2.5844(7) Å, respectively, and are longer by ca. 0.14 and ca. 0.05 Å than those in **3**, which may be compared with the difference of the ionic radii for Ti^{3+} (0.81 Å) and Ti^{4+} (0.75 Å),[38] although the

elongation of the Ti−S bond is somewhat more significant. The Ti−P and Ti−S bond lengths in **6** are similar to those in **5**.

Limited numbers of results have been reported for the crystallographic structures of the complexes with Ti(III)−phosphorus bonds to date, and the Ti(III)−phosphorus bond lengths in such complexes range from 2.46 to 2.70 Å.[26,39−51] Interestingly, the Ti(III)−P bond lengths in **5** and **6** are somewhat longer than the Ti(II)−phosphorus bond lengths in $(\eta^5\text{-MeC}_5\text{H}_4)_2\text{Ti}(\text{Me}_2\text{PCH}_2\text{CH}_2\text{PMe}_2)$ (2.527(4) and 2.540(4) Å)[52] and $\text{Cp}_2\text{Ti}(\text{PMe}_3)_2$ (2.524(4) and 2.527(3) Å),[53] despite the larger ionic radius of Ti^{2+} (1.00 Å) in the d^2 electronic configuration.[38] It seems that the back-donation from Ti(II) to the phosphorus atom is responsible for the short Ti(II)−P bond: the larger covalent character of Ti(II)−P than that of Ti(III)−P is indicated. In a similar way, the Ti(III)−P bond seems stronger than the bonding between Ti(IV) and P.

Complexes **5** and **6** are paramagnetic. The EPR spectrum of **5** in THF at room temperature exhibited an intense doublet signal due to ^{31}P with Ti satellites on both sides: $A(\text{P}) = 21.3$, $g = 1.991$. The spectrum of **6** under the same conditions was intense but broad: the g value was 1.990, although estimation of A(P) was not possible. These A(P) and g values are similar to those for $\text{Cp}_2\text{TiCl}(\text{PMe}_3)$ ($A(\text{P}) = 20.2$, $g = 1.986$ at room temperature) and for $\text{Cp}_2\text{TiMe}(\text{PMe}_3)$ ($A(\text{P}) = 20.2$, $g = 1.986$ at 263 K) for which coordination of PMe_3 is confirmed in solution,[54] indicating that the structures of **5** and **6** in the solid state are retained in THF solutions. Paramagnetic complexes **5** and **6** are very unstable (air sensitive), as indicated by the very low redox potential. Although the EPR parameters are not sensitive to contamination with diamagnetic Ti(IV) (air-oxidized species), the magnetic susceptibility is significantly influenced by contamination with such diamagnetic species. Therefore, we decided not to report unreliable magnetic parameters in this article, as it is difficult to avoid partial oxidation of Ti(III) during preparation of samples for the measurement of the magnetic susceptibility. Complexes **5** and **6** react with diphenyl disulfide (molar ratio = 1:1.5) to yield $\text{Cp}_2\text{Ti}(\text{SPh})_2$[55] along with other byproducts, which indicates that the relatively large Ti(III) center tends to suffer from an attack by diphenyl disulfide to allow oxidative addition.

An alternative synthetic procedure, on the basis of the method by Bochmann et al.[56] for the synthesis of $[\text{Cp*}_2\text{TiMe}(\text{THF})]\text{BPh}_4$ from $\text{Cp*}_2\text{TiMe}$, was also examined in this study. The dark green suspension of AgBPh_4 and 1 equiv of **5** or **6** in THF was stirred for 4 h to yield a dark purple-red solution with metallic silver. After removal of silver, the solvent was evaporated to dryness. Complexes **3** and **4** were successfully isolated from acetonitrile solutions of the residue in ca. 40% yields.

Heterobimetallic Complexes, $[\text{Cp}_2\text{Ti}\{\text{S}(\text{CH}_2)_{2\text{or}3}\text{PMe}_2\}_2\text{-M}]$. Attempts were made to prepare heterobimetallic complexes, following White and Stephan's method for $[\text{Cp}_2\text{Ti}(\text{SC}_2\text{H}_4\text{PPh}_2)_2\text{Cu}]\text{BF}_4$[15] and $[\text{Cp}_2\text{Ti}(\text{SC}_3\text{H}_6\text{PPh}_2)_2\text{Ni}]$:[17] dark red crystals of $[\text{Cp}_2\text{Ti}(\text{SC}_2\text{H}_4\text{PMe}_2)_2\text{Cu}]\text{PF}_6$ (**7**) were obtained from **1** (Scheme 1). While complex **7** was easily synthesized by the reaction of **1** with $[\text{Cu}(\text{CH}_3\text{CN})_4]\text{PF}_6$ in 84% yield, the preparation of other heterobimetallic complexes with Ni(II) or Fe(II) was not successful: reactions of **1** with $\text{NiCl}_2(\text{PPh}_3)_2$ and FeCl_2 gave Ni(dmpet)_2[6] (ca. 94% yield) and $\text{Fe}_3(\text{dmpet})_6\text{Cl}$ (ca. 59% yield), together with Cp_2TiCl_2. The structure of $\text{Fe}_3(\text{dmpet})_6\text{Cl}$ was clarified by X-ray analysis to be a linear trinuclear complex with two *fac*-$[\text{Fe(II)P}_3\text{S}_3]$ and one $[\text{Fe(III)S}_6]$ unit.[57] The reaction of **2** with Ni(cod)_2 (cod = 1,5-cyclooctadiene) produced only a trace amount of $[\text{Cp}_2\text{Ti}(\text{SC}_3\text{H}_6\text{PMe}_2)_2\text{Ni}]$, which is in contrast to the high yield of $[\text{Cp}_2\text{Ti}(\text{SC}_3\text{H}_6\text{PPh}_2)_2\text{Ni}]$[17] (70%). $[\text{Ni(dmppt)}_2]$ was isolated (ca. 50% yield) from the reddish brown mixture of **2** and Ni(cod)_2 in THF. Therefore, it seems that the $[\text{Ni}^{\text{II}}(\text{dmppt})_2]$ complex is the more stable than $[\text{Cp}_2\text{Ti}(\text{SC}_3\text{H}_6\text{PMe}_2)_2\text{Ni}]$, and the dissociation of dmppt from **2** took place upon mixing **2** and Ni(cod)_2. The reactions of **2** with FeCl_2 and $[\text{Fe}(\text{CH}_3\text{CN})_6](\text{ClO}_4)_2$ yielded $\text{Fe}_3(\text{dmppt})_6\text{Cl}$ and $[\text{Fe}_2(\text{dmppt})_3(\text{CH}_3\text{CN})_3](\text{ClO}_4)_2$, respectively. These reactions of **1** and **2** with metal ions indicate that the Ti(IV)−S bonds in **1** and **2** are readily cleaved by addition of late transition metal ions to form the more stable $[\text{M}_n(\text{dmpet or dmppt})_m]$ complexes.

The $^{31}\text{P}\{^1\text{H}\}$ NMR spectrum of **7** exhibited a singlet signal at −21.6 ppm: the notably small downfield shift ($\Delta = 29.3$ ppm) from the signal of free dmpet can be explained by the higher electron density on Cu(I) compared with that on Ti(IV) in **3** for which a large chemical shift of the $^{31}\text{P}\{^1\text{H}\}$

(38) Shannon, R. D. *Acta Crystallogr.* **1976**, *A32*, 751−767.
(39) Troyanov, S. I.; Meetsma, A.; Teuben, J. H. *Inorg. Chim. Acta* **1998**, *271*, 180−186.
(40) Chen, L.; Cotton, F. A.; Dunbar, K. R.; Feng, X.; Heints, R. A.; Uzelmeir, C. *Inorg. Chem.* **1996**, *35*, 7358−7363.
(41) Cotton, F. A.; Wojtczak, W. A. *Gazz. Chim. Ital.* **1993**, *123*, 499−507.
(42) Britten, J.; Mu, Y.; Harrod, J. F.; Polowin, J.; Baird, M. C.; Samuel, E. *Organometallics* **1993**, *12*, 2672−2676.
(43) Christou, V.; Wuller, S. P.; Arnold, J. *J. Am. Chem. Soc.* **1993**, *115*, 10545−10552.
(44) Binger, P.; Muller, P.; Philips, P.; Gabor, B.; Mynott, A. T.; Hermann, A. H.; Langhauser, F.; Kruger, C. *Chem. Ber.* **1992**, *125*, 2209−2212.
(45) Gomez, R.; Cuenca, T.; Royo, P.; Pellinghelli, M. A.; Tripicchio, A. *Organometallics* **1991**, *10*, 1505−1510.
(46) Fenske, D.; Grissinger, A.; Hey-Hawkins, E. M.; Magull, J. Z. *Anorg. Allg. Chem.* **1991**, *595*, 57−66.
(47) Samuel, E.; Mu, Y.; Harrod, J. F.; Dromzee, Y.; Jeannin, Y. *J. Am. Chem. Soc.* **1990**, *112*, 3435−3439.
(48) Jensen, J. A.; Wilson, S. R.; Girolami, G. S. *J. Am. Chem. Soc.* **1988**, *110*, 4977−4982.
(49) Razavi, A.; Mallin, D. T.; Day, R. O.; Rausch, M. D.; Alt, H. *J. Organomet. Chem.* **1987**, *333*, C48−C52.
(50) Jensen, J. A.; Girolami, G. S. *J. Chem. Soc., Chem. Commun.* **1986**, 1160−1162.
(51) Kool, L. B.; Rausch, M. D.; Alt, H. G.; Herberhold, M.; Wolf, B.; Thewalt, U. *J. Organomet. Chem.* **1985**, *297*, 159−169.
(52) Girolami, G. S.; Wilkinson, G.; Thornton-Pett, M.; Hursthouse, M. B. *J. Chem. Soc., Dalton Trans.* **1984**, 2347−2350.
(53) Kool, L. B.; Rausch, M. D.; Alt, H. G.; Herberhold, M.; Thewalt, U.; Wolf, B. *Angew. Chem., Int. Ed. Engl.* **1985**, *24*, 394−401.
(54) Samuel, E.; Henique, J. *J. Organomet. Chem.* **1996**, *512*, 183−187.
(55) Giddings, S. A. *Inorg. Chem.* **1967**, *6*, 849−850.
(56) Bochmann, M.; Jaggar, A. J.; Wilson, L. M.; Hursthouse, M. B.; Motrvalli. *Polyhedron* **1989**, *8*, 1838−1843.

(57) Crystal data for $[\text{Fe}_3(\text{dmpet})_6]\text{Cl}\cdot\text{CH}_2\text{Cl}_2$ prepared by different methods: $\text{C}_{25}\text{H}_{62}\text{S}_6\text{P}_6\text{Cl}_3\text{Fe}_3$, fw = 1014.87, space group $C2/m$, $a = 17.856(9)$ Å, $b = 10.101(7)$ Å, $c = 13.857(5)$ Å, $\beta = 111.46(4)°$, $V = 2326(2)$ Å^3, $Z = 4$, $D_{\text{calc}} = 2.898$ g cm^{-3}, μ(Mo Kα) = 31.75 cm^{-1}, $R = 0.047$, $R_{\text{w}} = 0.055$.

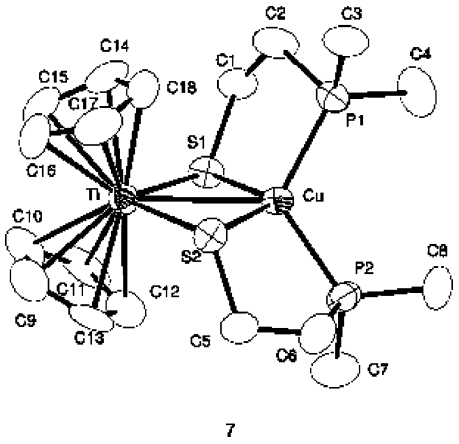

7

Figure 4. ORTEP drawings of **7** (Ti−Cu 2.95(1), Cu−S(1) 2.271(2), Cu−S(2) 2.292(10), Cu−P(1) 2.26(2), Cu−P(2) 2.24(2), Ti−S(1) 2.48(1), Ti−S(2) 2.467(5) Å, S(1)−Ti−S(2) 97.3(4), S(1)−Cu−S(2) 109.1(3), Ti−S(1)−Cu 76.6(3), Ti−S(2)−Cu 76.6(2), P(1)−Cu−P(2) 117.6(4)°).

signal was observed upon coordination (Δ = 73.5 ppm). A similarly small downfield shift (Δ = 21.3 ppm) of the ^{31}P-{^{1}H} signal was reported for $[Cp_2Ti(SC_2H_4PPh_2)_2Cu]BF_4$.[15]

The crystal structure of **7** was determined by X-ray analysis, and the ORTEP drawing of the cationic part of **7** is shown in Figure 4 with selected bond lengths and angles. The coordination geometry around the Cu center in **7** is a distorted tetrahedron with the dihedral angle between S1−Cu−S2 and P1−Cu−P2 planes being 70.0°. The Ti−S bond lengths (2.48(1) and 2.467(5) Å) in **7** are longer than those in Ti(IV) complexes **1** (2.390(2) and 2.383(3) Å) and **3** (2.3498(9) Å): they were rather close to the bond length of Ti−S (2.4877(7) Å) in Ti(III) complex **5**. The Ti−Cu distance (2.95(1) Å) in **7** is shorter by ca. 0.07 Å than that in analogous $[Cp_2Ti(SC_2H_4PPh_2)_2Cu]PF_6$ (3.021(1) Å),[15] along with the shorter Cu−S and Cu−P bond lengths in **7**. Furthermore, the average Ti−S−Cu bond angle (76.6(2)°) in **7** is slightly smaller than that (78.1(1)°) in $[Cp_2Ti(SC_2H_4PPh_2)_2Cu]PF_6$.

As the existence of metal-to-metal bonding has been suggested for $[Cp_2Ti(SC_2H_4PPh_2)_2Cu]PF_6$,[15] a similar dative interaction is also possible in complex **7**, by considering the shorter Cu−Ti distance in **7** than in $[Cp_2Ti(SC_2H_4PPh_2)_2Cu]PF_6$. In such a case, the Cu(I)(d^{10}) to Ti(IV)(d^0) dative bond seems to be more significant in **7** than in $[Cp_2Ti(SC_2H_4PPh_2)_2Cu]PF_6$, due to the larger electron density on Cu(I) in **7** than that in $[Cp_2Ti(SC_2H_4PPh_2)_2Cu]PF_6$. The difference in the electron density on Cu(I) is caused by the difference in the σ-donicity of the $-PMe_2$ donor sites in **7** and that of the $-PPh_2$ site in $[Cp_2Ti(SC_2H_4PPh_2)_2Cu]PF_6$. Therefore, the elongated Ti(IV)−S bonds in **7**, the bond length of which is similar to Ti(III)−S in **5**, seem to reflect the increased electron density on Ti(IV) in **7** through dative interaction with Cu(I).

CpTi(IV) and Cp*Ti(IV) Complexes with dmpet and dmppt. The reaction of Cp^*TiCl_3 with 3 equiv of Lidmpet produced complex **8** in a 63% yield, while the reactions with 1 or 2 equiv of Lidmpet resulted in the formation of unstable and uncharacterized products in a very low yield. On the other hand, the reaction of $CpTiCl_3$ with 1 equiv of Lidmppt produced complex **9** in 57% yield, while unknown products were obtained by the reactions with 2 and 3 equiv of Lidmppt.

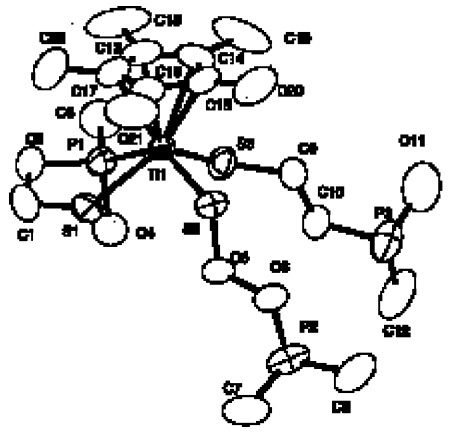

8

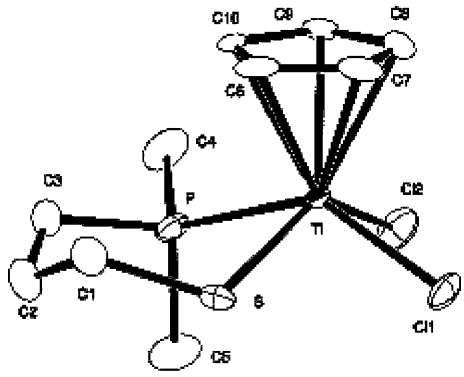

9

Figure 5. ORTEP drawings of **8** (Ti−S(1) 2.425(2), Ti−S(2) 2.339(1), Ti−S(3) 2.385(1), Ti−P 2.652(1) Å, S(1)−Ti−S(2) 82.98(5), S(1)−Ti−S(3) 124.23(5), S(2)−Ti−S(3) 93.49(5), S(1)−Ti−P(1) 72.65(4), S(2)−Ti−P(1) 135.89(5), S(3)−Ti−P(1) 72.33(4)°) and **9** (Ti−S 2.361(1), Ti−P 2.556(1), Ti−Cl(1) 2.342(1), Ti−Cl(2) 2.370(1) Å, S−Ti−P 80.15(4), Cl-(1)−Ti−Cl(2) 86.68(4), Cl(1)−Ti−S 82.33(4), Cl(2)−Ti−P 77.25(4)°).

The crystal structures of complexes **8** and **9** determined by X-ray analyses are shown in Figure 5 with selected bond lengths and angles. In complex **8**, only one of the three dmpet ligands coordinates to the Ti(IV) center in a κ^2S,P mode, while two other dmpet ligands bind to Ti(IV) only through S. It seems that the dmpet ligand with κ^2S,P coordination mode in **8** rather weakly binds to the Ti(IV) center: the Ti-(1)−S(1) bond length (2.425(2) Å) is very long compared with Ti(1)−S(2) (2.339(1) Å) and Ti(1)−S(3) (2.385(1) Å), while the lengths of the latter two bonds are comparable to those in complex **1** (2.390(2) and 2.383(2) Å) and complex **3** (2.3498(9) Å). Complex **9** has a structure similar to that of **8** with a dmppt ligand coordinated to Ti(IV) through P and S. The Ti−P(2.556(1) Å) and Ti−S(2.361(1) Å) bond lengths are shorter than those for the chelating dmpet in complex **8**. Such a difference in Ti−P and Ti−S lengths may reflect the sterically less demanding nature of Cp than Cp*.

The ^{1}H NMR signal at 1.12 ppm (doublet) observed at 20 °C for complex **8** (J_{PH} = 1.7 Hz, 18H, P(CH_3)$_2$) split into multiple signals at −80 °C in toluene-d_8, indicating that

Scheme 2

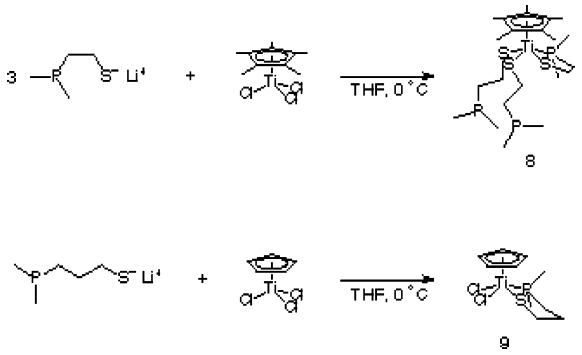

Scheme 3

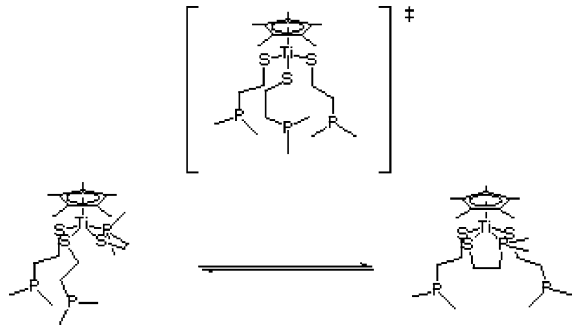

three distinct $-PMe_2$ moieties in two different coordination environments at −80 °C become indistinguishable at elevated temperatures: a rapid site-exchange between dmpet ligands in κ^2S,P and κS coordination modes takes place at room temperature (Scheme 3). To examine the rate of this site-exchange process, variable-temperature $^{31}P\{^1H\}$ NMR measurements in toluene-d_8 solution of **8** were carried out in the temperature range from −80 to 80 °C. A somewhat broad singlet signal was observed at −29 ppm at 80 °C. As the solution was cooled, the singlet signal broadened further and disappeared at 0 °C. However, three sharp singlet signals were observed at −80 °C at 17.5, −51.2, and −51.5 ppm with the intensity ratio of 1:1:1 (Figure 6). The resonance at 17.5 ppm was attributed to the coordinated phosphorus on dmpet in a κ^2S,P coordination mode, as the chemical shift is close to the value observed for complex **3**, 22.6 ppm. The two higher field signals were assigned to the two uncoordinated phosphorus atoms on the dmpet ligands in a κS coordination mode, as the chemical shifts of these two signals are almost identical to those for complex **1**.

By using the DNMR v4.1.0 program,[58] the line shapes of the NMR spectra at each temperature were calculated and fitted to the experimentally obtained $^{31}P\{^1H\}$ NMR spectra in order to evaluate the rate constants for the mutual site-exchange process and the corresponding activation parameters: $k_{ex}^{298} = 1.9 \times 10^5\ s^{-1}$, $\Delta H^{\ddagger} = 48\ kJ\ mol^{-1}$, and $\Delta S^{\ddagger} = 17\ J\ mol^{-1}\ K^{-1}$. No exchange sequence other than the mechanism shown in Scheme 3 reproduced the experimental spectral change: the exchange process must involve dissociation of the Ti(IV)−P bond.

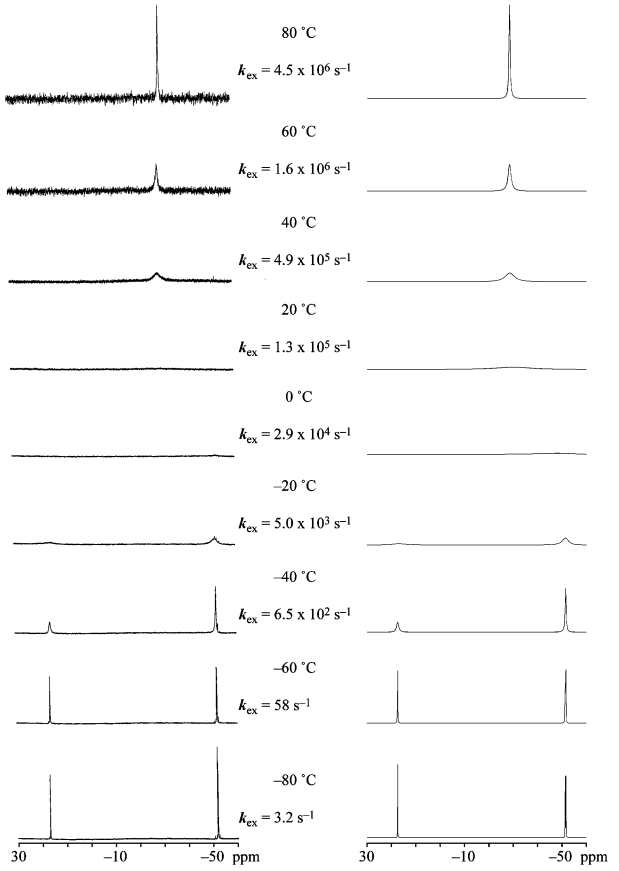

Figure 6. Dynamic NMR measurements: $^{31}P\{^1H\}$ NMR spectra of **8** in toluene-d_8 at −80 to 80 °C. Calculated NMR spectra at each temperature are shown in the right column, together with the best-fit values of the rate constants.

As it is known that a coordination number of more than 6 is common for Ti(IV), a mechanism through the associative transition state may be possible for the mutual site-exchange reaction observed in this study.[59] On the other hand, the relatively long Ti(IV)−P bond may indicate dissociative activation for this reaction. Traditionally, the reaction mechanisms for solvent exchange and/or ligand substitution reactions (intramolecular mutual site-exchange process is also included in this category) have been elucidated either from the dependence of the observed rate constant on the concentration of the entering ligand (by means of rate law), by comparing the obtained activation parameters with those for other known reactions, or through discussions on the characteristics of entering and leaving donor sites.[60] However, such a classical method for elucidating reaction mechanisms of the solvent exchange/site-exchange processes may not be valid any more:[60] recent calculations by Cooper and Ziegler confirmed[61] that even in the solvent exchange and ligand substitution reactions of d^8 Pt(II), for which the reaction has long been believed to proceed through the associative mechanism, the contribution of the dissociation mode to the activation process is significant (>90%) although the ex-

(58) The GNMR4 program was modified to work on a Macintosh computer. The original program was "Program for Iterative Analysis of Exchange Broadened NMR Spectra" by David. S. Stephenson and Gerhard Binsch, Munich, 1978.

(59) Greenwood, N. N.; Earnshaw, A. *Chemistry of the Elements*, 2nd ed.; Butterworth: Oxford, U.K., 1997.

(60) Jordan, R. B. *Reaction Mechanisms of Inorganic and Organometallic Systems*, 2nd ed.; Oxford University Press: Oxford, U.K., 1998.

(61) Cooper, J.; Ziegler, T. *Inorg. Chem.* **2002**, *41*, 6614−6622.

perimentally observed exchange and substitution rates obviously depended on the concentration of the entering ligand. On this basis, most of the exchange/substitution processes on metal complexes in solution may be dissociative in nature, and the *apparent* dependence of the observed rate constant on the individual characteristics and the concentration of each entering ligand is explained by the concerted nature of the exchange/substitution processes. Moreover, the crystal structure of complex **8** confirms that the large thiol moieties as well as the bulky Cp* ligand provide a coordinatively saturated environment around the Ti(IV) center: the Ti−P bond is long (2.652(1) Å) and the bite angle of the chelating dmpet ligand is rather small (72.33(4)°). We, therefore, conclude that the intramolecular mutual site-exchange reaction within complex **8** is regarded to proceed through the dissociation of coordinated P atom on the chelating dmpet ligand. Then the activation enthalpy, $\Delta H^{\ddagger}$, is a measure of the Ti(IV)−P bond strength in complex **8**: the relatively small activation enthalpy of this reaction is certainly related to the long Ti(IV)−P bond length in **8**.

The ^{1}H NMR signal at 6.56 ppm (doublet, 5H, C_5H_5, $J_{PH} = 2.4$ Hz) and the $^{31}P\{^{1}H\}$ signal at 13.22 ppm observed for complex **9** in chloroform indicate that the coordination of dmppt to Ti(IV) through P and S atoms observed in the crystal is retained in solution. The shorter Ti(IV)−P and Ti(IV)−S bond lengths in **9** than those in **8** ensure resistance to dissociation of the dmppt ligand in **9**: the Ti(IV)−P bond is shorter in **9** than in **8**, since (1) the smaller steric demand of chloride ions than the dangling P−S moiety in **8** and (2) the less bulky nature of the Cp ring compared with Cp* provide sufficient space around Ti(IV) for tighter Ti−P bonding in **9**.

Conclusion

We reported nine novel titanium complexes bearing hybrid bidentate ligands with sulfur and dimethyl-substituted phosphorus as donor atoms in this study. It was found that Ti(IV) tends to bind more strongly to the S^- moiety than to $-PMe_2$. The Ti(IV)−P bonds in complexes **3**, **4**, **8**, and **9** were unequivocally longer than the Ti(IV)−S bonds, reflecting the inferior basicity of the phosphorus donor site to the S^- moiety. However, the Ti(IV)−P bond lengths in these complexes were shorter than those for the other complexes reported to date, probably because of the sterically less demanding nature of $-PMe_2$. We also reported novel isostructural Ti(IV)/Ti(III) pairs with hybrid P−S ligands, complexes **3**/**5** and **4**/**6**, although the redox potential for the **3**/**5** couple was rather low. However, the difference in the Ti(III)−P and Ti(IV)−P bond lengths was merely 0.04 Å, while the Ti−S lengths in complexes **5** and **6** were some 0.14−0.17 Å longer than those in complexes **3** and **4**. Such a small elongation of the Ti−P bond may be explained by the stabilization of the Ti(III)−P bond through π back-bonding, while it seems that the large elongation of the Ti−S bond directly reflects the decrease of the electronic charge on the central metal ion. The weak nature of the Ti(IV)−P interaction was also demonstrated by the rapid mutual site-exchange reaction in complex **8**.

Acknowledgment. This work was supported in part by a Grant-in-Aid for Scientific Research on Priority Areas (No. 14078101, 14078211 "Reaction Control of Dynamic Complexes") from the Ministry of Education, Culture, Sports, Science, and Technology, Japan, and H.D.T. expresses his thanks to the Kurata Foundation, Hitachi Corp, for financial support.

Supporting Information Available: Lists of X-ray crystallographic files, in CIF format, are available free of charge via the Internet at http://pubs.acs.org.

IC034353L